1997 HST Calibration Workshop
Space Telescope Science Institute, 1997
S. Casertano, et al., eds.

Calibrating the WFPC2 Astrometry for MDS

Kavan U. Ratnatunga, Eric J. Ostrander, and Richard E. Griffiths

Department of Physics, Carnegie Mellon University, Pittsburgh, PA 15213

Abstract.

The HST Medium Deep Survey has optimized an automated procedure to associate and stack WFPC2 data. The coordinates listed in HST WFPC2 image and/or jitter file headers are often found to be insufficient to stack images for cosmic ray removal. We discuss results from software developed for the HST Medium Deep Survey (MDS) pipeline to evaluate these shifts by cross-correlation of the images. We will also discuss the distortion of the pre-cool-down WFPC2 field and attempts to derive absolute coordinates for MDS WFPC2 observations using the USNO-A1.0 half billion object catalog.

1. Introduction

The Hubble Space Telescope (HST) Medium Deep Survey (MDS) Key Project (Griffiths et al. 1994) includes pure parallel observations of a large number of random fields extending over multiple years and focuses on the statistical properties of all measurable objects. The processed MDS database in September 1997 is about 500 fields (one square degree) with well over one hundred thousand objects. The MDS database has been made available on the MDS web-site in the HST archive (`http://archive.stsci.edu/mds`) and also mirrored at the Canadian Astronomy Data Center CADC (`http://cadcwww.dao.nrc.ca/mds`). Much effort in the MDS project was devoted to developing a pipeline for associating and stacking WFPC2 data (Ratnatunga et al. 1995). An automated procedure was required, not only for practical considerations of processing a very large number of both pure parallel and archival fields, but also to maintain uniformity in the statistical properties of the MDS database. These improvements are particularly important for quantitative analysis of the faintest extended sources with low signal-to-noise.

Images were originally stacked using WFPC2 image header information or jitter files when available. However some of the resulting stacks which looked acceptable to the "eye", gave unexpected results when the images were analyzed using the 2-dimensional image analysis procedure developed for the MDS (Ratnatunga et al. 1997). In a well stacked field, jitter and any small errors in the tinytim PSF used in the analysis results in a "half-light radius" estimate for stellar images which are typically about 20 mas or 0.2 of a WFC pixel. Stellar images were well resolved from extended galaxy images with half-light radius larger than about half a pixel. However, in few of the fields stellar images yielded a half-light radius estimate of about one WFC pixel. Comparison of magnitudes in such a field with another overlapping field also highlighted a serious problem in the stacking.

2. Estimating Shifts Between Images

A study of these stacks showed that the problem was caused by errors of order one WFC pixel in the shifts derived from the jitter file headers (.jih). The jitter file information was assumed to be more reliable since they are derived from the engineering telemetry

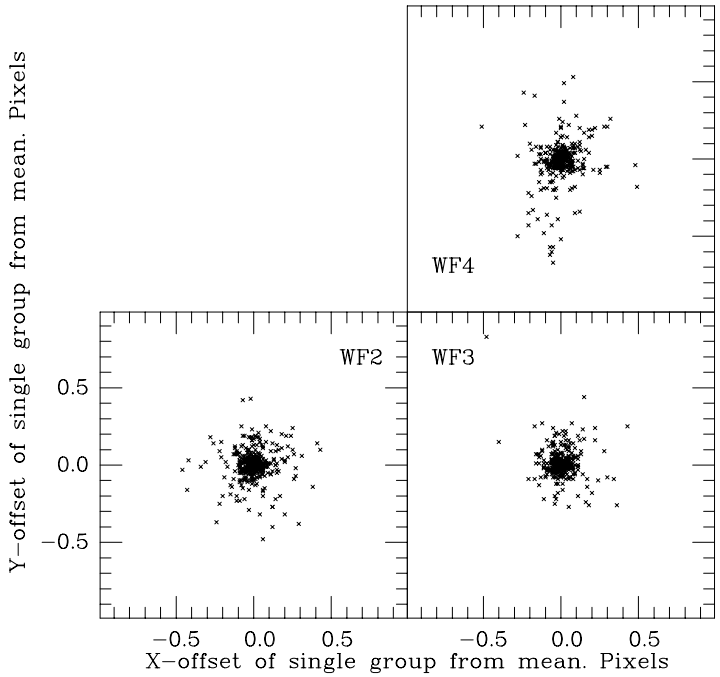

Figure 1. Consistency of shifts estimated for individual WFPC2 chip relative to the mean for datasets in dithered stacks. The slightly larger vertical scatter in WF4 maybe caused by the many bad columns in that CCD. The size of the region shown is one pixel.

taken during the observation, rather than from the requested coordinate which is put in the WFPC2 raw data file (.d0h) header.

It was not practical to determine the shifts interactively for a very large number of fields using IRAF/STSDAS. Cross-correlation was the only hope of determining these shifts by an automated procedure. The image cross-correlation algorithm needs to operate on unstacked, calibrated data, allowing for the presence of cosmic rays which outnumber and are much brighter than the faint galaxy and stellar images in the pure parallel fields. Also of concern are masked columns of bad pixels, hot pixels and the occasional saturated stellar images which could distort the cross-correlation.

A cross-correlation is derived independently for each of the three WFC CCD chips rotated to the WFC-4 orientation. Cross-correlations with very poor signal are ignored. The weighted sum of the acceptable cross-correlation is used to derive the adopted shift for the dataset. Consistency between the shifts for each the individual groups in comparison to the total gives measure of reliability. All stacks in the full MDS database have been checked and any field that may have suffered from poor stacking has been reprocessed.

We will not go into the details of the algorithm (any interested reader should contact the first author), but illustrate the results. The difference between the adopted shift for the dataset and the shift from each individual WFPC2 chips is less than half a pixel with an rms of under a tenth of a pixel as shown by the crosses in figure 1.

We can investigate the magnitude of the shift errors by considering only the most reliable datasets which gave consistent (within half-pixel) shift for all groups. We see in figure 2 that only the information from the jitter files for non-dithered primary observations can be assumed to be reliable. Shift errors for dithered observations are significantly larger

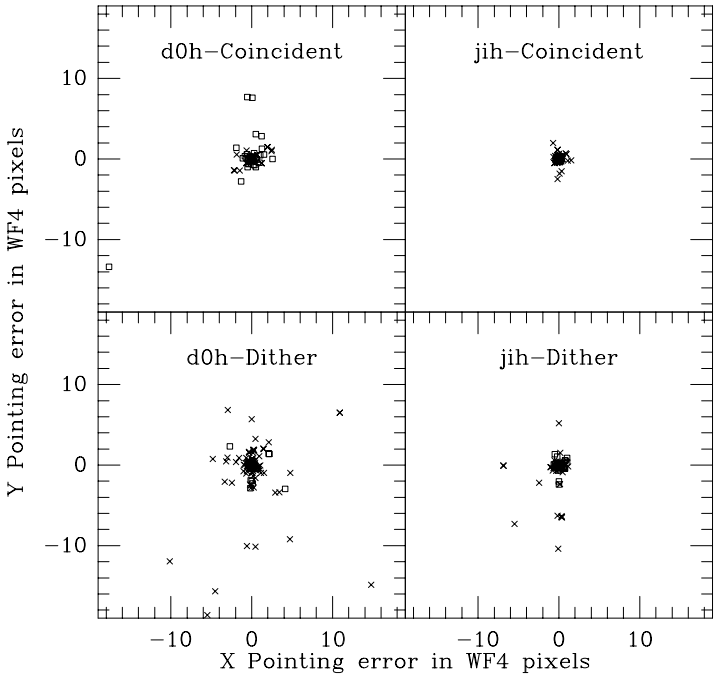

Figure 2. The relative shift errors between WFPC2 Datasets. Symbols indicate observation type: Parallel (cross); Primary (square)

than for coincident observations (see table-1). The error is also larger for pure parallel observations over similar primary observations.

Table 1. RMS shift errors between HST WFPC2 Datasets.

Type of Observation		.d0h header Info. Number of datasets	x rms Pixels	y rms Pixels	.jih jitter Info. Number of datasets	x rms Pixels	y rms Pixels
Parallel	Coincident	893	0.22	0.15	552	0.17	0.23
Primary	Coincident	330	1.28	1.50	55	0.08	0.10
Parallel	Dither	193	4.32	4.53	116	1.09	1.75
Primary	Dither	170	0.51	0.51	113	0.28	0.39

These errors, which result from coordinate errors in the guide stars and the mapping of the FGS, are not unexpected. Dithered images require the guide stars to be at different location of the FGS, and the derived coordinates then suffer from any error in the mapping of the FGS. "Peakups" in the primary observation could give unpredictable pointing shift in the related pure parallel observation. These errors would need to be recognized when stacking STIS and particularly NICMOS pure-parallel observations. This would be a harder task than for WFPC2 to solve by cross-correlation since the number of observed objects in the limited field of view is much smaller. If a broad-band WFPC2 observation is available in parallel, it could probably be used to constrain the shifts in the primary pointing during the observation.

3. WFPC2 Pre-cool-down Distortion Map

The largest strip of uniformly observed WFPC2 fields (Groth et al. 1994) was taken before the detector was cooled down from $-78\,\mathrm{C}$ to $-88\,\mathrm{C}$ on April 23, 1994. The WFPC2 distortion mapping derived from F555W observations taken after cool-down was found to be inadequate for these pre-cool-down data. The difference is most probably caused by the change in temperature.

The IDT WFPC2 distortion map derived from globular cluster ω Cen observations has 20 coefficients for each CCD giving a total of 80 for the camera (Holtzman et al. 1995). Since these coefficients don't represent physical parameters it is not easy to correct or investigate to determine the changes required for pre-cool-down data. In the absence of sufficient pre-cool-down data to constrain a mapping of 80 coefficients, a simpler model with 7 parameters for each CCD was used. The selected 7 parameters and the parameter identification used in Table 2 are:

- (1) [g2] The pixel scale in arc seconds
- (2) [s2] Coefficient of the main quadratic term in the distortion.
- (3,4) [xc,yc] coordinates of the center of the distortion map in pixels. This is close but not exactly at the central [400,400] pixel of each WFPC2 CCD chip.
- (5,6) [x0,y0] coordinates the CCD chip origin from metric reference in arc seconds.
- (7) [th] Orientation of the CCD in degrees. These are the differences from the nominal rotation angles, multiples of 90°, and are less than $0\overset{\circ}{.}5$.

The adoption of the Cartesian metric aligned with the orientation of the PC chip and using reference pixel WF3 [133,149] as the origin removes three parameters. The MDS WFPC2 distortion model has therefore only 25 free parameters, rather than the 80 coefficients used in the Holtzman et al. (1995) distortion map.

To derive the coefficients we selected the 28 Groth-Westphal strip fields and 5 other fields observed before April 1994 which overlap. The selection and orientation of the overlap are not ideal for deriving the distortion, but we had to use what was readily available. To constrain the relative pointing on a scale larger than the WFPC2 an iterative procedure was used to identify objects in each field which have coordinates in the USNO-A1.0 catalog of a half billion objects in the sky. This catalog is very useful since it is currently the only catalog which will ensure at least a few objects in each WFPC2 field. On average one could expect 25, but the number will clearly be strongly dependent on Galactic latitude. At Galactic latitude +60°, corresponding to the Groth-Westphal, strip we found on average 3 objects in each WFPC2 field. In addition to the reference stars we cross-identify objects in the MDS catalogs in the overlapping regions of the fields.

A global maximum likelihood solution was derived. The model included the 25 parameters for the WFPC2 distortion map and 3 free parameters for each WFPC2 field included in the solution. For example, when 33 fields are used there are a total of $25 + 3 * 33 = 124$ free parameters. The likelihood function assuming Gaussian errors is integrated over the USNO-A reference stars and the coordinates of cross-identified object in the field-overlap regions. The errors of the WFPC2 centroids was provided by the MDS Maximum Likelihood image analysis software (Ratnatunga et al. 1997). We adopt a $0\overset{''}{.}3$ rms error for the USNO-A1.0 coordinates (Monet et al. 1996).

Preliminary solutions with error estimates for both before and after the WFPC2 cool-down in wide band filters F606W and F814W are given on Table 2. A single iteration is used to reject any cross-identification which shows a very large ($> 5\sigma$) residual and could be suspected to be a false identification. Hardly any of the USNO-A identifications are

Table 2. MDS WFPC2 distortion model coefficients

			Pre-cool-down				Post-cool-down			
			F814W-78c		F606W-78c		F814W-88c		F606W-88c	
		WFPC2 Fields	33		30		31		20	
		USNO-A stars	135(135)		84(84)		582(582)		285(287)	
		MDS Crossids	1416(1525)		1399(1441)		6159(6576)		3474(3603)	
G	id	units		+/-		+/-		+/-		+/-
1	[1]	g2 mas	45.422	0.028	45.330	0.035	45.498	0.013	45.449	0.020
2	[1]	s2 5.E-9	6.49	0.90	6.76	0.82	8.52	0.69	7.71	1.05
3	[1]	xc pixel	365.0	13.7	375.1	18.9	376.7	8.2	396.3	18.5
4	[1]	yc pixel	364.0	15.7	350.0	14.1	391.1	7.4	386.4	11.1
F	[1]	x0 arcsec	8.214		8.327		8.031		8.054	
F	[1]	y0 arcsec	7.947		8.066		7.721		7.804	
F	[1]	th degree	0.000		0.000		0.000		0.000	
5	[2]	g2 mas	99.451	0.053	99.237	0.075	99.480	0.013	99.441	0.022
6	[2]	s2 5.E-9	6.71	0.68	6.81	1.12	7.05	0.14	7.90	0.19
7	[2]	xc pixel	334.2	10.5	320.5	14.8	385.2	1.7	382.3	2.0
8	[2]	yc pixel	408.2	8.8	416.6	30.3	408.7	2.1	440.2	5.1
9	[2]	x0 arcsec	12.766	0.020	12.879	0.033	12.625	0.007	12.664	0.019
10	[2]	y0 arcsec	5.207	0.010	5.339	0.009	5.089	0.006	5.099	0.017
11	[2]	th degree	0.505	0.009	0.506	0.009	0.500	0.007	0.504	0.010
12	[3]	g2 mas	99.288	0.050	99.070	0.067	99.450	0.013	99.380	0.022
13	[3]	s2 5.E-9	7.52	0.67	7.57	1.08	6.90	0.13	7.04	0.20
14	[3]	xc pixel	425.7	8.2	420.3	28.1	408.7	2.0	453.3	5.6
15	[3]	yc pixel	453.9	10.2	454.1	18.4	399.7	1.6	391.9	2.3
16	[3]	x0 arcsec	13.348	0.046	13.315	0.069	13.347	0.006	13.384	0.019
17	[3]	y0 arcsec	14.856	0.043	14.823	0.066	14.829	0.006	14.811	0.017
18	[3]	th degree	0.189	0.008	0.194	0.008	0.186	0.007	0.200	0.011
19	[4]	g2 mas	99.455	0.066	99.168	0.086	99.462	0.014	99.376	0.039
20	[4]	s2 5.E-9	8.87	1.24	7.63	1.47	6.62	0.15	6.91	0.26
21	[4]	xc pixel	413.1	12.5	419.2	15.8	393.8	1.5	392.6	3.2
22	[4]	yc pixel	378.2	7.3	367.8	31.9	403.8	1.8	395.6	8.9
23	[4]	x0 arcsec	5.556	0.067	5.683	0.091	5.234	0.006	5.272	0.013
24	[4]	y0 arcsec	14.557	0.071	14.675	0.118	14.587	0.007	14.739	0.012
25	[4]	th degree	-0.280	0.047	-0.368	0.102	-0.369	0.007	-0.376	0.014

The metric coordinates (xm,ym) in arc-seconds for [G][xobs,yobs]
from reference pixel [3][133,149] is given by the FORTRAN code

```
theta = mod(G-1,4)*pi/2. - th(G)/(180./pi)
x  = xobs - xc(G)
y  = yobs - yc(G)
r2 = x*x + y*y
xt = g2(G)*(xc(G)+(1.0d0 - 5.E-9*s2(G)*r2)*x)
yt = g2(G)*(yc(G)+(1.0d0 - 5.E-9*s2(G)*r2)*y)
xm = x0(G) + xt*cos(theta) - yt*sin(theta)
ym = y0(G) + xt*sin(theta) + yt*cos(theta)
```

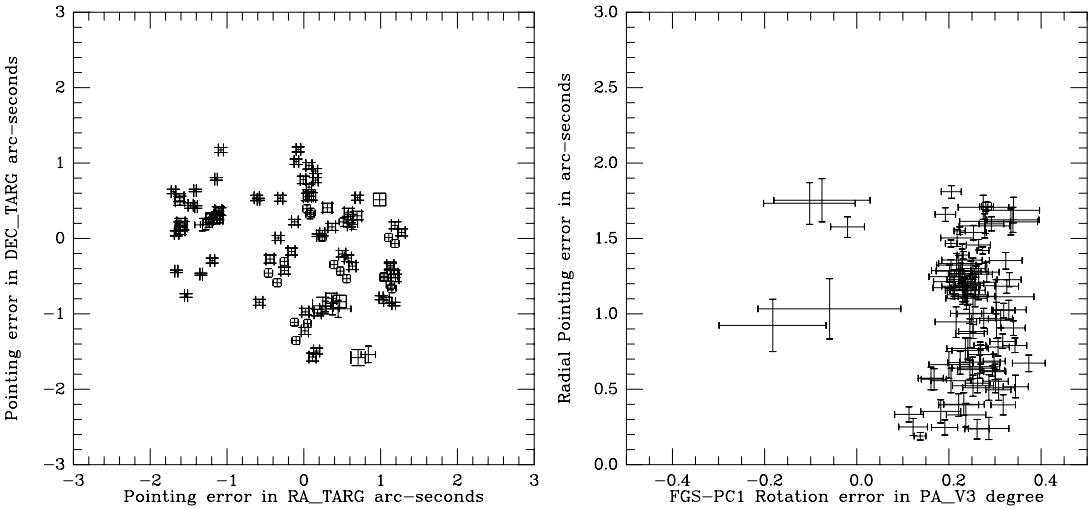

Figure 3. Accuracy of HST pointing.

rejected. However about 2% of the MDS cross-identifications are rejected. The number before rejection is given in parenthesis in Table 2.

We note that the plate scale has changed significantly between post and pre-cool-down models. A small decrease in the plate scale is also apparent between F814W and F606W filters.

The pre-cool-down solution decreases the χ^2 by a factor of 10 over using the standard Holtzman et al. (1995) solution on these data. The comparable accuracy post-cool-down solution is 20% better than the χ^2 derived adopting the Holtzman solution *for these data*. This was unexpected, considering the large decrease (80 to 25) in the number of parameters used in the distortion model. However, in order to avoid image analysis close to regions with rapid changes to the PSF and image distortion, the MDS catalogs filtered out objects with centroids within 10 pixels of edges of the pyramid and CCD. The more flexible Holtzman distortion map is probably required in these regions. The model would need to be used on the original ω Cen data used to derive the Holtzman et al. (1995) calibration for an objective comparison. Our simpler model, with physically understandable parameters, will anyway be useful to monitor any changes in the distortion over time. This has not been done yet, and the software is available to the STScI or any other user interested in following up on this issue.

4. Accuracy of HST Pointing

The solutions discussed above also provides an estimate for the correction to the HST coordinates of the WFPC2 pointing and orientation (PA_V3). The coordinate differences are shown on the left in Figure 3. On the right we show the radial error and the error in the PA_V3 orientation. The mean pointing error is about 1 arc-second. There appears to be a systematic relative difference of 0.°3 between the adopted standard (PA_V3−135.0) from the FGS and the orientation of the PC1 chip of the WFPC2. This error is comparable to the difference from right-angle rotations of the WFPC2 CCD chip orientations. The FGS system appears to be closer to the orientation of WF4 chip.

Estimates will be made for all of the HST pointings after the USNO-A2.0 or the GSC2 catalogs are made available referenced to the new global HIPPARCOS coordinate frame (Perryman et al. 1997). The current systems referenced to the much smaller FK5 catalog

are known to have systematic errors of order 1.0 arc seconds in few regions of the sky, comparable to the random errors of the HST pointing. Accurate absolute coordinates are needed for spectroscopic follow-ups and are useful to cross-identify objects in overlapping fields and ensure they are assigned the same coordinate identification.

5. Conclusion

WFPC2 image cross-correlation software was developed to derive relative shifts between WFPC2 observations. The shifts are derived independently for each WFPC2 group and are consistent to within 0.1 pixels rms.

We find that dithered observations and parallel observations have larger pointing errors relative to coincident and primary observations.

A simple, 25-parameter WFPC2 distortion map has been derived for pre-cool-down observations at $-78\,\mathrm{C}$, and yields a χ^2 10 times smaller than the post-cool-down solution of Holtzman et al. (1995) on these data. Post-cool-down solutions have also been obtained for both F814W and F606W.

The mean pointing accuracy of the HST WFPC2 using the GSC1.1 catalog and the current FGS mapping appears to be about $1''$. A systematic difference of $0\overset{\circ}{.}3$ is measured between the FGS (PA_V3−135) and the PC1 orientation.

Acknowledgments. This paper is based on observations with the NASA/ESA Hubble Space Telescope, obtained at the Space Telescope Science Institute, which is operated by the Association of Universities for Research in Astronomy, Inc., under NASA contract NAS5-26555. The Medium Deep Survey is funded by STScI grant GO2684 and daughters. We also thank USNO and CADC for making the large USNO-A catalog searchable over the World Wide Web.

References

Griffiths, R. E., et al., 1994, ApJ, 437, 67

Groth, E. J., Kristian, J. A., Lynds, R., O'Neil, E. J., Balsano, R., & Rhodes, J., 1994 BAAS, 26, 1403

Holtzmann, J. A., et al., 1995 PASP, 107, 156

Monet, D., et al., 1996 in *USNO-A 1.0* Flagstaff: USNO

Perryman, M. A. C., et al., 1997, in *The Hipparcos and Tycho Catalogues* (Noordwijk: ESA), 1, 311

Ratnatunga, K. U., Griffiths, R. E., Neuschaefer, L. W., & Ostrander, E. J. 1995, Proc. *HST Calibration Workshop II*, eds. A. Koratkar and C. Leitherer (Baltimore: STScI), 351

Ratnatunga, K. U., Griffiths, R. E., & Ostrander, E. J., 1997, in preparation